

# Sensor-Response-Ratio Constancy Under Changes in Natural and Artificial Illuminants

Javier Romero,\* Daniel Partal, Juan L. Nieves, Javier Hernández-Andrés

Facultad de Ciencias, Departamento de Óptica, Universidad de Granada, Granada 18071, Spain

Received 3 May 2006; revised 16 September 2006; accepted 18 October 2006

*Abstract:* We have analyzed the constancy of the response ratio for cones, second-stage mechanisms, and CCD sensors when daylight or an artificial illuminant (A, F2, F7, and F11) is changed to an equal-energy illuminant (E) in scenes containing natural and artificial objects. The response ratios were always found to be roughly constant for all the sensors. For daylight, we have deduced mathematical expressions, which relate the values of these ratios with the correlated color temperature (CCT) and applied these expressions to the synthesis of images of a scene viewed under different daylights corresponding to a variety of CCTs. The results were highly satisfactory in a rural scene for any CCT. In the scene with artificial objects, the results were also good for nonextreme CCTs. We also included in our study artificial illuminants, with which we achieved very good image syntheses for illuminants A and F7. © 2007 Wiley Periodicals, Inc. *Col Res Appl*, 32, 284–292, 2007; Published online in Wiley InterScience (www.interscience.wiley.com). DOI 10.1002/col.20329

*Key words:* illuminants; color imaging; color constancy

## INTRODUCTION

The spectral composition of the light that reaches the eye of an observer from an object is given in mathematical terms by the product of the spectral-power distribution (SPD) of the light source illuminating the object and the spectral reflectance of the object. When this light arrives at the retina, the cones generate electric signals, which—after their transmission and processing by other types of

neurons in the retina and in the brain—give rise to color perception. If the light source changes, whether in intensity or spectral composition, the light reflected by the object also changes and in consequence so do the final values of the cone excitation.

Different authors<sup>1–5</sup> have found a linear relationship with a high correlation coefficient representing, for a broad set of objects, the pairs of excitation values for each cone ( $L$ ,  $M$ , or  $S$ ) determined for each object under two different illuminants. This linear relationship indicates that the ratio of the excitations under illuminant changes for each type of cone remains roughly constant for all objects. The concept can be expressed mathematically as

$$\frac{L'}{L''} = \alpha; \quad \frac{M'}{M''} = \beta; \quad \frac{S'}{S''} = \gamma \quad (1)$$

where ( $L'$ ,  $M'$ ,  $S'$ ) and ( $L''$ ,  $M''$ ,  $S''$ ) are the excitation values of the cones for the same spectral reflectance under two different illuminants and ( $\alpha$ ,  $\beta$ ,  $\gamma$ ) are values that depend upon the illuminants alone.

The constancy of the ratios of the cones has been tested for illuminant pairs that include daylight, illuminant E, illuminant A, and Planckian illuminants, both with natural objects as well as artificial ones. This result has been used as an argument to help explain the phenomenon of color constancy.<sup>2,4,6</sup> This refers to the apparent persistence of the perceived color of an object regardless of the changes in the illumination under which it is observed, an object observed in daylight and then under incandescent light for example. Colorimetrically, the color of an object changes, but the color perceived may remain the same. Many theories seek to explain this phenomenon, including those that search for neuronal mechanisms behind the descriptors of object color invariant to illumination changes.<sup>7</sup> von Kries' theory<sup>8</sup> adopts the same mathematical form as that of the expressions in Eq. (1). Foster and Nascimento<sup>2</sup> indicated

\*Correspondence to: Javier Romero. (e-mail: jromero@ugr.es)

Contract grant sponsor: Comisión Interministerial de Ciencia y Tecnología, Spain; contract grant number: DPI 2004-03734.  
© 2007 Wiley Periodicals, Inc.

that the constancy of the cone-excitation ratios may be related to a gain mechanism at the receptor level, which largely explains the experimental results found on measuring color constancy.

Other authors,<sup>1,4</sup> instead of looking for invariant descriptors, point to the existence of mechanisms in the human visual system that make it possible to detect illumination changes in the same object, although the color perceived might be different. That is, mechanisms that can recognize whether the colorimetric changes in a scene are due to an illumination change or whether the object itself has changed. Furthermore, in these cases, the constancy in the cone ratios may be a possible key to enabling the visual system to recognize an object regardless of illumination changes. With this in mind, Foster and Nascimento<sup>2</sup> pointed “the traditional interpretation of color constancy is formally equivalent to one based on discriminating illuminant changes from nonilluminant changes (operational approach).”

When the responses of the second-stage mechanisms were analyzed,<sup>3,4</sup> the behavior found was similar to that of cone excitation. These authors showed that the affine relationships can be established between the values of the color-opponent mechanisms (yellow-blue and red-green) when the illumination changes. Nieves *et al.*<sup>9</sup> also found these relationships experimentally. The affine relationships present additive terms that Zaidi *et al.*<sup>3</sup> found in the red-green mechanism, Nieves *et al.*<sup>9</sup> in both opponent mechanisms.

Analyzing the results of these different authors,<sup>2,4,5</sup> we can deduce that the slope of the straight-line fit representing cone-excitation values under two illuminants or, equivalently, the values of  $\alpha$ ,  $\beta$ , and  $\gamma$  in Eq. (1), varied with the change in the illuminants. Nevertheless, no search seems to have been made to date to find a mathematical expression to predict the values for certain illuminant changes. Our first aim therefore was to find a relationship between the values of  $\alpha$ ,  $\beta$ ,  $\gamma$ , and the CCT of daylight, for which the daylight SPD is characterized by this parameter alone.<sup>10,11</sup> Thus, we determined the value of the slopes for the representations of the excitation of each cone on changing daylight to illuminant E. We then looked for mathematical expressions that predicted the values of the cone ratios for each CCT with which we could predict the cone ratios for different daylights and also simulate scenes viewed under these illuminants, where the cone-ratio constancy is exact. This study was widened to include the mechanisms of the second-stage: achromatic, yellow-blue, and red-green.

We also tried to discover whether the cone ratio remains constant when dealing with artificial illuminants. Some authors<sup>1,2</sup> have studied Planckian illuminants, including illuminant A. In our case, we widened our study to fluorescent illuminants (F2, F7, and F11), for which the SPDs present peaks typical of this type of source. Borges<sup>12</sup> showed that type (1) relationships are almost exact when the illuminants are white with soft SPDs. We tested SPDs that diverged substantially from this situation,

although the chromaticity coordinates fell within the zone of the achromatic or white illuminants of the chromaticity diagram.

If the relationships between the cone-excitation values of the expressions in Eq. (1) are fulfilled for a certain group of illuminants, we will have a method of calculating the values  $L'$ ,  $M'$ , and  $S'$  corresponding to an object under a given illuminant when having only the values of  $L''$ ,  $M''$ , and  $S''$  generated by the same object with the equal-energy illuminant. In daylight, a scene under natural illumination of a certain CCT can be simulated at another CCT. In the second part of our work, images taken under natural illumination are compared with others made by simulation on applying the expressions in Ref. 1 and the formulas deduced for  $\alpha$ ,  $\beta$ , and  $\gamma$ . In this way, we can calculate the colorimetric differences between a real scene and a simulated one in which the ratio of the cone-excitation values is completely constant.

Some authors<sup>13,14</sup> have evaluated other ways of predicting cone-excitation values when the illuminant changes. Funt and Lewis<sup>13</sup> found no advantages in using signals generated by second-stage mechanisms compared to using the cone-excitation values directly, and even more so when the spectral sensitivities of the cones were sharpened.<sup>15</sup> This latter result might be expected, as West and Brill<sup>16</sup> have demonstrated that narrower spectral-sensitivity sensors improve the validity of von Kries transformations. Finlayson *et al.*<sup>15</sup> also found that sharpening the sensors improved the results of von Kries predictions.

In addition, Finlayson *et al.*<sup>14</sup> showed that other prediction methods of cone signals (nondiagonal transformations) achieve better results than von Kries transformations. It is not our aim here, however, to identify the best prediction method for cone-excitation values under illuminant changes but rather to study the validity of the linear fittings made on establishing constant relationships in cone excitation, and to evaluate whether the errors that occur in the prediction based on type (1) transformations are sufficiently small for this method to be applied with assurance. The advantages of applying the linear transformation include its easy application, its low computational cost and its direct relationship with receptor gain mechanisms present in color vision.

The question immediately arises as to whether what has been studied for the cones ( $L$ ,  $M$ ,  $S$ ) is valid for another set of three sensors ( $R$ ,  $G$ ,  $B$ ) corresponding to an artificial system such as a CCD camera. To solve this, we studied the constancy of the ratio of the signals generated by these types of sensor, taking as an example the sensors of a commercial CCD camera. The results were applied once more to the synthesis of images for the different CCTs with natural as well as artificial illuminants. As pointed out by other authors,<sup>17</sup> in computer-graphic design, the color ( $R_s^0$ ,  $G_s^0$ ,  $B_s^0$ ) of an object illuminated by a certain source is often calculated directly by multiplying the value of the illuminated object by that of the equal-energy illuminant ( $R_E^0$ ,  $G_E^0$ ,  $B_E^0$ ) and the corresponding values of a perfectly white object illuminated under this

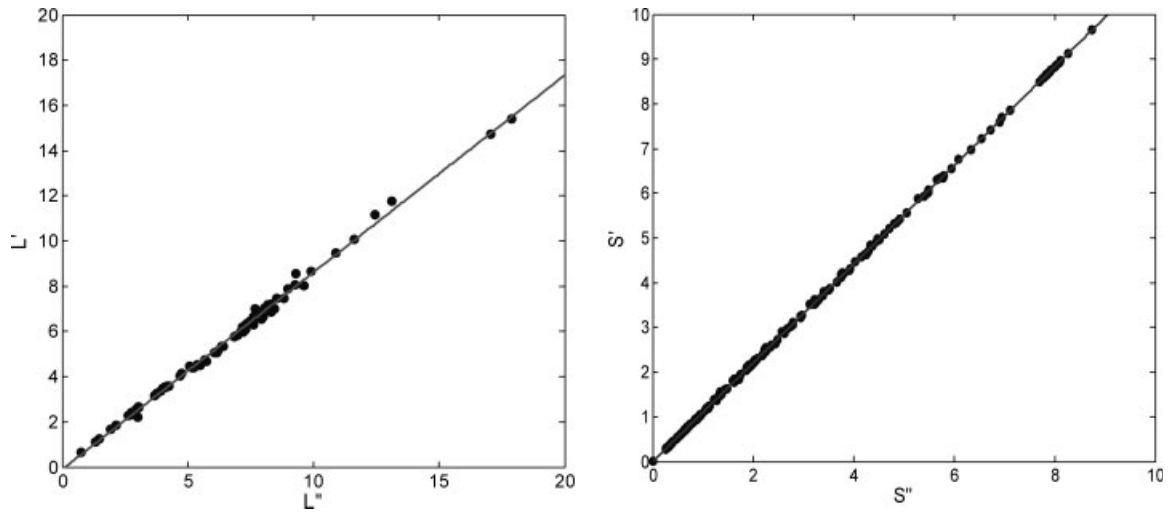


FIG. 1. Examples of linear fittings for cone signals of objects viewed under a test illuminant ( $y$ -axis) and illuminant E ( $x$ -axis). Left: L cone, test illuminant F2, natural objects. Right: S cone, test illuminant daylight (CCT 150 mireds), artificial objects.

source ( $R_s^w, G_s^w, B_s^w$ ). This represents a major saving in computation time of the images. The mathematical terms are

$$R_s^0 = R_E^0 R_s^w; \quad G_s^0 = G_E^0 G_s^w; \quad B_s^0 = B_E^0 B_s^w \quad (2)$$

For this assumption to be exact, it must fulfill the constancy of the ratio of the signals generated by the sensors when changing the illumination between the objects of illuminant E to the illuminant under which the scene is to be simulated. This means that an analysis of the exactitude of the ratio constancy of the signals generated by the sensors should serve to determine the validity of these image-synthesis methods.

Drew and Finlayson<sup>17</sup> developed a prediction method based on the representation by linear models of the spectral reflectances of objects and color signals (the product of the spectral reflectance and the SPD of the illuminant)

and the sharpening of the eigenvectors belonging to the representational basis. Their results improve upon those obtained with von Kries transformations and furthermore avoid the metamerism of the illuminant that this type of transformation cannot predict, since from the expressions in Eq. (1) it can be deduced that metameric pairs of objects observed under one illuminant will continue to be metamers under another illuminant. This will be a limitation of the method used in this research as it is in the usual methods applied to computer graphics. Nevertheless, the limited number of objects, especially natural ones, which might involve metamerism is outweighed by the simplicity of the calculation in the prediction of the sensor excitation values.

It is worth emphasizing that we are seeking to test the validity of the simple transformations of the type expressed in Eq. (1) to study the prediction possibilities

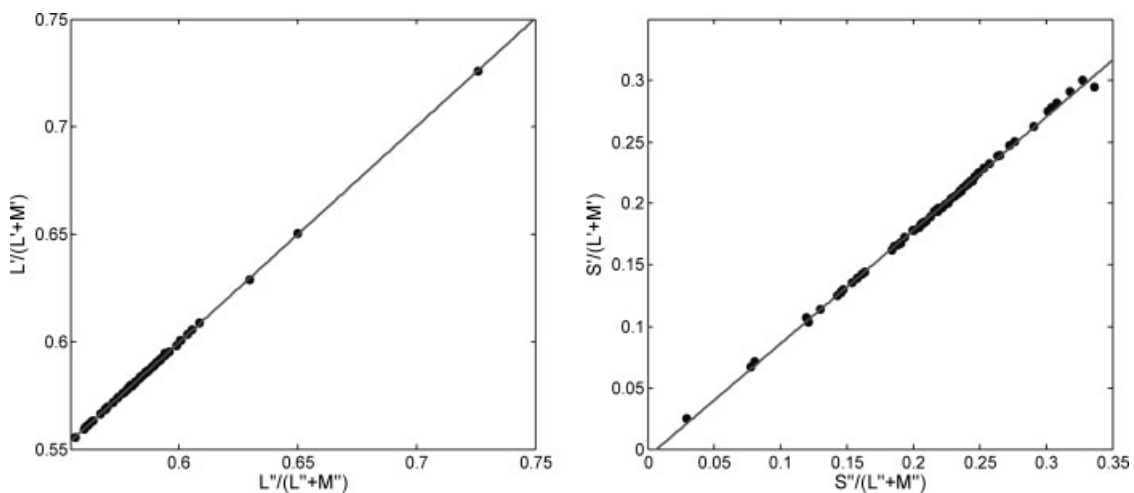


FIG. 2. Examples of linear fitting for second-stage-mechanism signals of objects viewed under a test illuminant ( $y$ -axis) and illuminant E ( $x$ -axis). Left:  $L/(L + M)$ , test illuminant daylight (CCT 199.5 mireds), natural objects. Right:  $S/(L + M)$ , test illuminant daylight (CCT 150 mireds), natural objects.

TABLE I. Cone-signal ratios, second-stage-signal ratios, and square-correlation coefficients of the linear fittings for artificial illuminants and artificial objects.

	F2		F7		F11		A	
	Ratio	$R^2$	Ratio	$R^2$	Ratio	$R^2$	Ratio	$R^2$
$L$	0.874	0.998	1.069	0.998	4.975	0.998	1.055	0.997
$M$	0.838	0.993	1.125	0.999	4.703	0.995	0.955	0.998
$S$	0.564	0.999	1.165	0.999	3.044	0.999	0.657	0.999
$L/(L + M)$	0.791	0.991	0.925	0.997	0.928	0.984	1.032	0.994
$S/(L + M)$	0.957	0.955	1.059	0.998	0.948	0.935	0.807	0.975
$(L + M + S)$	0.792	0.992	1.111	0.977	4.443	0.954	0.930	0.948

under daylight changes from a single CCT datum of the light and to analyze new illuminants, such as fluorescent illuminants. If we establish the conditions under which a von Kries transformation generates results that make the simulated scene colorimetrically almost indistinguishable from the original, we will have a simple method for synthesizing images and one which is easier to understand than other more elaborate algorithms.

#### OBJECTS AND ILLUMINANTS

We selected a set of spectral reflectances of natural and artificial objects, a set of daylight and artificial illuminants, and a set of multispectral images. The spectral reflectances for the artificial objects were the 240 chips of the Macbeth Color-Checker,<sup>18</sup> whilst those of the natural objects (71 in total) were from the set measured by Vrhel *et al.*<sup>19</sup>

We selected 22 daylight SPDs measured by members of our laboratory,<sup>11</sup> which correspond to clear and cloudy days, from sunrise to sunset, covering the CCT daylight range between 3757 and 32754 K. The 22 SPD daylight objects presented CCTs of 266 to 30.5 mireds, selected at intervals of  $\sim 10$  mireds. Tominaga and Wandell<sup>20</sup> showed that the color temperature scale in mired units is visually more uniform than in Kelvin, thus justifying our selection

of daylight SPDs. All the SPDs were normalized to unity at 560 nm.

The artificial illuminants studied were illuminant A and the fluorescent illuminants F2, F7, and F11, following CIE recommendations.<sup>21</sup> This selection enabled us to work with some of the most representative illuminants of conventional artificial sources. The SPDs of these illuminants were also normalized to unity at 560 nm.

The multispectral images used in the second part of our work were selected from the set of images supplied by Nascimento *et al.*<sup>5</sup> This set of images contains rural scenes, urban scenes, and interiors with artificial objects. We derived the spectral reflectance from each pixel of each image, and were thus able to determine the color signals by simply multiplying the SPD of the illuminant to be used to simulate the scene.

The spectral-reflectance and SPD values were used at intervals of 5 nm over a range of 400–700 nm. To calculate the cone-excitation values of  $L$ ,  $M$ , and  $S$ , we used the fundamentals of Smith and Pokorny.<sup>22</sup>

#### CONE-SIGNAL RATIO AND DEPENDENCE UPON CORRELATED COLOR TEMPERATURE

Figure 1 presents some examples of the fittings made on representing the cone-excitation values for a certain illuminant and a set of objects against those determined for

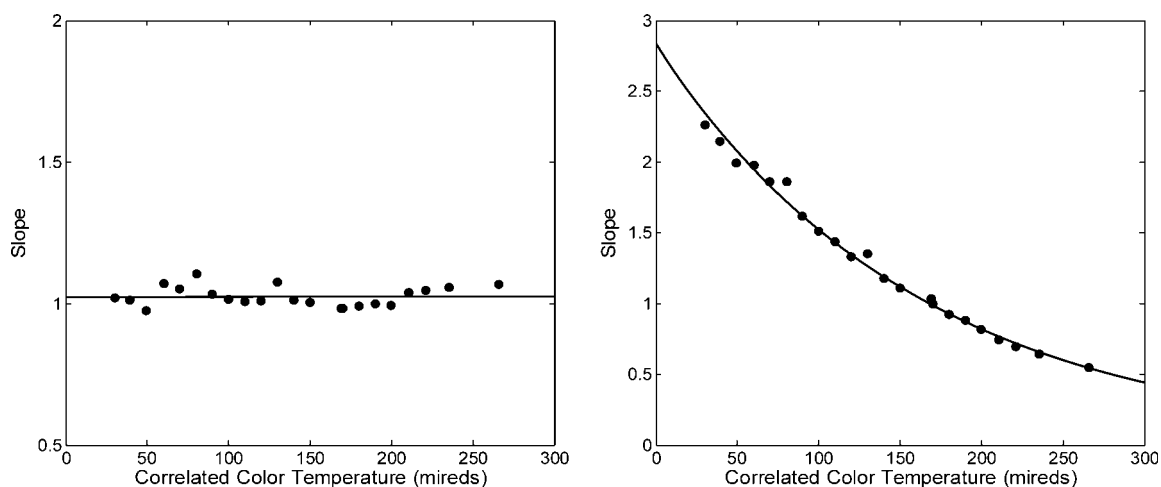


FIG. 3. Examples of graphical representations of signal ratios (slopes of linear fittings) against daylight CCT. Left:  $L/(L + M)$ , natural objects. Right:  $S$  cone, natural objects.

TABLE II. Mathematical expressions that relate the dependence of different cone- and second-stage-signal ratios and the correlated color temperature of daylight.

Mechanism	Objects	Mathematical expression	$R^2$
$M$	Natural	$ER = 1.28 \exp(-0.0013 \text{ CCT})$	0.931
	Artificial	$ER = 1.30 \exp(-0.0013 \text{ CCT})$	0.935
$S$	Natural	$ER = 2.83 \exp(-0.0062 \text{ CCT})$	0.995
	Artificial	$ER = 2.84 \exp(-0.0063 \text{ CCT})$	0.994
$S/(L + M)$	Natural	$ER = -0.0059\text{CCT} + 2.00$	0.992
	Artificial	$ER = -0.0028\text{CCT} + 1.42$	0.986
$(L + M + S)$	Natural	$ER = 1.41 \exp(-0.0019 \text{ CCT})$	0.950
	Artificial	$ER = 1.46 \exp(-0.0021 \text{ CCT})$	0.960

CCT, correlated color temperature in mireds; ER, excitation ratio;  $R^2$ , square-correlation coefficient.

illuminant  $E$ . Figure 2 offers the same type of representation but this time for the values generated in the mechanisms of the second stage ( $L/(L + M)$ ,  $S/(L + M)$ ,  $L + M + S$ ). We have used these expressions to represent second-stage mechanisms, as is usually done,<sup>3-5</sup> following MacLeod-Boynton's representation. As can be seen, the straight-line fitting to the data is quite good for daylight, as has also been indicated by other authors.<sup>1-5</sup> The same is true for illuminant A and the fluorescent illuminants. The  $R^2$  coefficients (square of correlation coefficient  $R$ ) found for the straight-line fittings to the values of  $L$ ,  $M$ , and  $S$  are better than 0.99 with all the illuminants and objects studied, both natural and artificial.

For the values of  $L/(L + M)$  and  $(L + M + S)$ , the  $R^2$  coefficients found surpass 0.99 for daylight CCTs higher than 70 mireds (i.e., excluding twilight<sup>11</sup>) and for the artificial illuminants in some cases (for artificial objects and illuminants F2, F7, and A, in the case of  $L/(L + M)$ ). With the other artificial illuminants and daylight CCTs lower than 70 mireds, the values found for the  $R^2$  coefficients were consistently higher than 0.97.

For  $S/(L + M)$ , the  $R^2$  coefficient was 0.99 for daylight, except for artificial objects and CCTs that were either very high or very low, and for the illuminant F7. In the remaining cases, the  $R^2$  coefficients were invariably above 0.93.

The additive term found in the regression straight lines was very close to zero in all cases. For example, for the CCT of 169 mireds (6250 K), the values of this parameter for  $L$ ,  $M$ , and  $S$  were  $-0.060$ ,  $-0.026$ , and  $0.005$ , respectively. This, together with the high linear correlation between the signals generated under each pair of illumi-

nants, indicates that the ratio of these signals is practically constant for the different objects and that the type (1) expressions appear to be quite valid. The possible affine representation to the changes in the signals generated in the red-green and yellow-blue opponent mechanisms predicted by Zaidi<sup>4</sup> and Nieves *et al.*<sup>9</sup> would give additive terms of very low values. For example, for the CCT of 169 mireds (6250 K), the values of this parameter for  $L/(L + M)$  and  $S/(L + M)$  were 0.001 and 0.005 respectively. It can be seen in Fig. 2 that these additive terms appear although with very low values.

In general terms, we can say that the ratios of the cone signals and the mechanisms of the second-stage signals remain constant with the daylight changes, except for the latter in the case of lights with extreme CCTs, in which constancy is lost somewhat. It is also noteworthy that the cone ratios remain constant for artificial illuminants with regard to illuminant  $E$ . For these types of illuminants, constancy declines when the mechanisms of the second stage are studied, except for illuminant F7, for which this decline is very slight. Table I shows the values for the excitation ratios of the different mechanisms for the artificial illuminants studied.

For daylight, we studied the dependence of the slope of the straight lines (excitation ratios) upon the CCT. To this end, we used conventional regression methods, which allowed us to determine the expression (whether linear or not) of the highest correlation coefficient relating the excitation ratios to the CCT. We found that for  $L$  and  $L/(L + M)$  a correlation could not be established between the values of the ratio of these signals and the daylight CCT, even though this parameter varies little from the CCT. The ratio of the  $L$ -signal had average and standard deviation values of 1.007 and 0.032, respectively, for natural as well as artificial objects. For  $L/(L + M)$ , these values were 0.996 and 0.032 (artificial objects) and 1.025 and 0.035 (natural objects). Thus, the  $L$  or  $L/(L + M)$  signals can be considered as hardly changing for daylight compared to their values for the equal-energy illuminant. For the rest of the first- and second-stage mechanisms, we found linear or exponential dependence of the slope upon the CCT. Figure 3 shows some examples of the results. The differences between the results for each set of reflectances (natural or artificial objects) were minimal, except for  $S/(L + M)$ . Table II gives the expression that resulted in each case. On adjusting, these mathematical expressions the  $R^2$  coefficients turned out to be especially good (greater than 0.99) for  $S$ . The reason may be the

TABLE III. Percentile values for the CIELAB color difference when comparing the original rural scene with that synthesised using the expressions in Table II.

Percentage	266.1 mireds (3757 K)	199.5 mireds (5013 K)	150 mireds (6668 K)	100.1 mireds (9992 K)	49.5 mireds (20,183 K)	30.5 mireds (32,754 K)
50	2.67	0.31	0.31	0.55	1.24	2.75
75	3.78	0.51	0.77	1.23	2.36	4.67
95	4.80	1.17	1.53	1.97	3.18	5.97

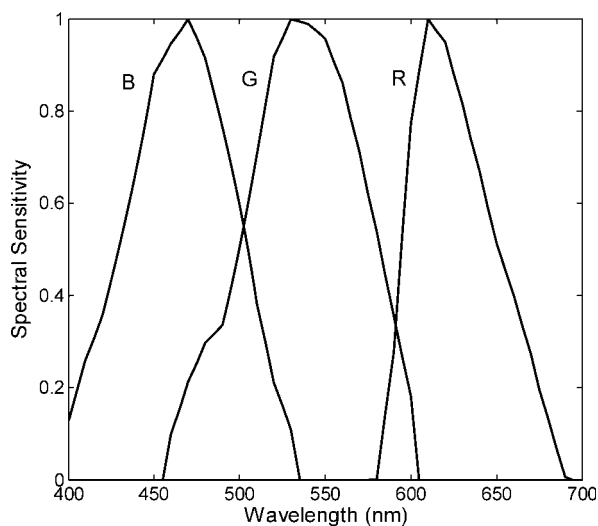


FIG. 4. Spectral sensitivity of the CCD sensors.

yellow-blue variation in daylight chromaticity during the day.<sup>11</sup> These results coincide with those of Lovell *et al.*,<sup>23</sup> who demonstrated that the color variation of objects during the day is supported fundamentally by the yellow-blue mechanism, while the red-green one remains almost unaltered.

In the case of the  $M$  cone, the  $R^2$  coefficients (the expression shown in Table II) exceeded 0.93, which, though not optimum, indicates a certain degree of correlation.

To test the validity of the expressions found for the dependence of the cone ratio upon daylight CCT, a natural scene under a given natural illumination of a certain CCT was colorimetrically compared to that found on transforming the same scene under equal-energy illumination to another that resulted from applying the expressions in Table II. That is, the  $L$ ,  $M$ , and  $S$  values of each pixel of the scene under equal-energy illumination were multiplied by the corresponding factors calculated from the expressions for the CCT of the scene to be simulated (Table II). The scene used, one of the multispectral images supplied by Nascimento *et al.*,<sup>5</sup> is categorized as rural.

The original scene under six daylight illuminants of CCTs of 266.1, 199.5, 150, 100.1, 49.5, and 30.5 mireds was compared to that simulated the aforementioned method. This comparison was made by calculating pixel by pixel the CIELAB color difference and determining

TABLE IV. CCD sensor-signal ratios and square-correlation coefficients of the linear fittings for artificial illuminants and artificial objects.

	F2		F7		F11		A	
	Ratio	$R^2$	Ratio	$R^2$	Ratio	$R^2$	Ratio	$R^2$
R	0.607	0.995	0.852	0.999	5.063	0.996	1.307	0.999
G	0.795	0.991	1.133	0.999	4.365	0.994	0.923	0.999
B	0.511	0.999	1.116	0.999	2.717	0.999	0.696	0.999

the percentiles in each case. To this end, we transformed the  $L$ ,  $M$ , and  $S$  values of each pixel in each image to  $L^*$ ,  $a^*$ , and  $b^*$  values and then calculated the color difference pixel by pixel. The color-difference values were determined at percentiles of 50, 75, and 95. The results are listed in Table III, where the CCT values are also presented in Kelvin for readers more accustomed to that scale. If, like other authors,<sup>17,19</sup> we consider up to three CIELAB units admissible when comparing samples of color scenes, we find that the results are very good for nonextreme CCTs, that is, normal ones in the middle of the day, but excluding twilight. Even at a temperature of 20183 K, the results can be considered satisfactory, this CCT corresponding to a sunset daylight SPD. The results worsen for extreme light at a temperature of 3757 K, which corresponds to a daylight SPD on a day with excessive dust in the atmosphere. Consequently, it may be said that the results are satisfactory as long as we wish to simulate natural scenes with illumination that covers most of the day, excluding twilight or unusual environmental conditions.

The expressions formulated to represent the dependence of the cone ratios upon the CCT were therefore adequate for simulating natural scenes under different illuminants. As a result, we may also conclude that for natural scenes, in which the natural illumination presents a nonextreme color temperature, the constancy in the cone ratio remains almost perfect, and this may help to explain color constancy under these illumination conditions.

#### SYNTHESIS OF IMAGES WITH ARTIFICIAL SENSORS

The results for the cone-excitation ratios under illuminant changes suggest the possibility of expanding the study to the synthesis of images when artificial sensors are used. We might expect that, for artificial sensors, the constancy of the von Kries relationships equivalent to the cone-signal ratios would remain or even improve. As indicated earlier, West and Brill<sup>16</sup> showed that sensors of narrower spectral sensitivity improve the validity of the Von Kries transformations, and this is usually for the sensors with which the image-acquisition and reproduction systems are equipped. Figure 4 shows the spectral sensitivity of the RGB sensors of a commercial camera and, as can be

TABLE V. Mathematical expressions that relate the dependence of the G and B sensor ratios and the correlated color temperature of daylight.

Sensor	Objects	Mathematical expression	$R^2$
G	Natural	$ER = 1.40 \exp(-0.0017CCT)$	0.948
	Artificial	$ER = 1.42 \exp(-0.0018CCT)$	0.949
B	Natural	$ER = 2.67 \exp(-0.0055CCT)$	0.993
	Artificial	$ER = 2.68 \exp(-0.0055CCT)$	0.993

CCT, correlated color temperature in mireds; ER, excitation ratio;  $R^2$ , square-correlation coefficient.

TABLE VI. Percentile values for the CIELAB color difference when comparing an original scene with that synthesised using expressions of Table V.

Percentage	266.1 mireds (3757 K)	199.5 mireds (5013 K)	150 mireds (6668 K)	100.1 mireds (9992 K)	49.5 mireds (20,183 K)	30.5 mireds (32,754 K)
Rural scene						
50	1.03	0.49	0.44	0.36	0.73	0.52
75	1.43	0.63	0.58	0.58	1.04	0.98
95	1.72	0.73	0.69	0.78	1.27	1.28
Interior scene						
50	3.08	1.45	1.27	1.17	2.24	1.66
75	4.12	1.84	1.62	2.03	3.10	3.11
95	9.14	2.38	2.36	4.19	6.42	8.41

seen, they are slightly narrower than those of the LMS cones and more widely spaced in the visible spectrum.

The linear fittings made earlier were repeated with the same objects and illuminants to determine the constancy ratios between the signals generated in each sensor on changing the illuminant. The correlation coefficients improved in all cases. Thus, for the changes between the equal-energy illuminant and the daylight-type illuminant, all the  $R^2$  coefficients were above 0.99 and were consistently higher than 0.999 for the  $R$  and  $B$  sensors. In the case of the  $G$  sensor, the  $R^2$  coefficients were of this order for daylight CCTs higher than 100 mireds.

With the artificial illuminants (Table IV) the results improved upon those found for LMS (Table I) for illuminants A and F7. The ordinates at the origin were in all cases close to zero.

When we studied the possible mathematical relationships that, for natural light, link the slope of the fittings, the signal ratio, and the daylight CCT, the results were similar to those found with the cones. Again the best fittings were found for the most sensitive sensor at short wavelengths, in this case  $B$ , with square-correlation coefficients of 0.99. For sensor  $G$ , the correlation was weaker, with a regression coefficient of 0.94, and very weak for sensor  $R$ . The mathematical expressions and the square-correlation coefficients are set out in Table V. These results were applied to the synthesis of images with these sensors, in the case of two multispectral images supplied by Nascimento *et al.*<sup>5</sup> One of the images was the rural scene used in the previous section and the second was an interior scene with artificial objects (toys). In this case, we add the scene with artificial objects because of the interest that this research might have in the synthesis of images in computer graphics, where artificial objects are so common. The CIELAB color differences were calculated pixel by pixel between the original image under a certain illuminant, established by multiplying the reflectance of each pixel by the daylight SPD, and the image resulting on applying to the image for the equal-energy illuminant the mathematical expressions that give the signal ratios of the sensors as a function of daylight CCT.

Table VI shows the results in terms of the different percentiles calculated. The results proved excellent for the rural scene, showing an improvement on those in Table

III. As far as the scene with artificial objects is concerned, the results were also very good for daylight at the mid hours of the day, excluding abnormal weather conditions.

As can be deduced from the results, the synthesis of images assuming the signal-ratio constancy, as is often done in computer graphics, is a good approach from the colorimetric standpoint. Our additional contribution is a method to achieve the synthesis of images while knowing only the daylight CCT to be simulated. This, as can be seen, gives very good results in rural scenes and even in scenes with artificial objects, while the CCTs are the usual ones for the mid hours of the day.

With the artificial illuminants, we calculated the color differences between the original interior scene (toys) and those found by multiplying that corresponding to the equal-energy illuminant by the slopes of the linear fitting (Table IV). The results are shown in Table VII, where it can be seen that for illuminants A and F7, the synthesis of the images can be considered colorimetrically very satisfactory. For the other two fluorescent illuminants, F2 and F11, the results are not so good. Although the  $R^2$  coefficients found for these illuminants in the linear fitting made to establish the signal ratio (Table IV) are apparently good (closer than 0.99), the established criterion for estimating the goodness of synthetic images is very demanding: color differences of less than three CIELAB units in more than 95% of the pixels, which would require square-correlation coefficients close or equal to 0.999. In Figure 5, we show two examples of histograms for the CIELAB color-difference values for the interior scene. In both cases, the simulated scenes are colorimetrically indistinguishable from the original ones for nearly all the pixels.

TABLE VII. Percentile values for the CIELAB color difference when comparing the original interior scene with that synthesised using the ratios in Table IV.

Percentage	F2	F7	F11	A
50	2.86	0.39	3.08	0.79
75	5.57	0.76	4.12	1.76
95	13.02	3.17	9.14	2.88

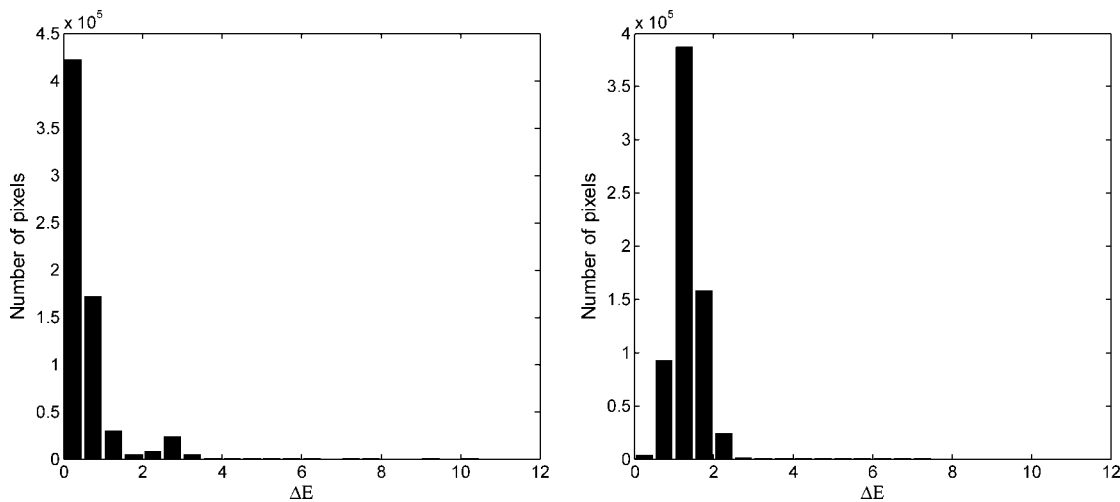


FIG. 5. Examples of histograms for CIELAB color-difference values when comparing original and synthesized images with CCD sensors. Left: interior scene, illuminant F7. Right: interior scene, daylight with CCT of 150 mireds.

### CONCLUSIONS

The cone-excitation ratios studied upon changing the equal-energy illuminant to another type of daylight or artificial light have been found to be roughly constant in all cases. The  $R^2$  coefficient of the linear fittings was consistently greater than 0.99. In the case of daylight, the results were highly satisfactory as were those for the constancy of the excitation ratios of the second-stage mechanisms, except for the SPDs of CCTs lower than 70 mireds or very high CCTs (twilight or abnormal atmospheric conditions). The results for the second-stage mechanisms for illuminant F7 were also satisfactory.

We studied the dependence of the cone ratio and of the second-stage-mechanism ratio with the CCT of daylight. The correlation between the ratio of the  $S$  cones and of the  $S/(L + M)$  mechanism and CCT was very high, because of the variations of daylight with CCT occurring in the yellow-blue direction of the chromatic diagram.<sup>11,23</sup> The correlation was weak for the  $M$  cone and absent for the  $L$  cone and the red-green mechanism ( $L/(L + M)$ ), although the variation in the ratios of these mechanisms with CCT was very slight.

The quantitative results of our research, that is, the values of the cone and second-stage-mechanism ratios and the parameters in the mathematical expressions, depend upon the normalization made of the illuminants; if the absolute values of the SPDs change, so do the excitation ratios. But the results remain qualitatively equal: the high degree of constancy for the excitation ratios for all the illuminants with respect to the equal-energy illuminant, and the high degree of correlation for  $S$  and  $S/(L + M)$  ratios and the CCT of daylight.

The simulations of natural scenes undertaken using the mathematical expressions deduced for the dependence of the excitation ratios of the different mechanisms upon the daylight CCT provided good results from the colorimetric point of view in natural scenes so long as the CCT was not extreme. It can be stated that in these scenes the

maintenance of the cone ratio was such that no significant color differences were appreciated with simulated scenes in which this ratio was presented with exactitude. This could help to explain the phenomenon of color constancy under natural illumination changes.

When we studied the possibilities of applying these same methods to the synthesis of images made with artificial sensors, we found again that for some sensors of the type used in CCD cameras the signal ratios remained constant and even improved with respect to those provided by the cones. This is linked to the fact that this type of sensor presents a narrower spectral sensitivity than that of the cones, thus improving the viability of the Von Kries transformations. The results of synthesizing natural images from the expressions obtained that linked the signal ratios to daylight CCT were very good in a rural scene, for any CCT. In the scene with artificial objects, the results were also satisfactory for nonextreme CCTs.

In the case of artificial illuminants, we achieved very good image synthesis for the illuminants A and F7. In these cases, the images synthesized from the deduced signal ratios reproduced scenes with artificial objects without significant color differences.

With our results, we seek not only to establish the limits of the application of the usual methods of generating color in computer graphics for certain natural and artificial illuminants, but also to provide a way of obtaining images synthesized with natural illumination, simply by fixing the daylight CCT to be simulated.

1. Dannemiller JL. Rank orderings of photoreceptor photon catches from natural objects are nearly illuminant-invariant. *Vision Res* 1993; 33:131–140.
2. Foster DH, Nascimento SMC. Relational colour constancy from invariant cone-excitation ratios. *Proc R Soc Lond B* 1994;257:115–121.
3. Zaidi Q, Spehar B, DeBonet J. Color constancy in variegated scenes: Role of low-level mechanisms in discounting illumination changes. *J Opt Soc Am A* 1997;14:2608–2621.



4. Zaidi Q. Identification of illuminant and object colors: Heuristic-based algorithms. *J Opt Soc Am A* 1998;15:1767–1776.
5. Nascimento SMC, Ferreira FP, Foster DH. Statistic of spatial cone-excitation ratios in natural scenes. *J Opt Soc Am A* 2002;19:1484–1490.
6. Nascimento SMC, Foster DH. Detecting natural changes of cone-excitation ratios in simple and complex coloured images. *Proc R Soc Lond B* 1997;264:1395–1402.
7. Hurlbert A. Computational models in color constancy. In: Walsh V, Kulikowski J, editors. *Perceptual Constancies; Why Things Look As They Do*. Cambridge, UK: Cambridge University Press; 1998. p 283–322.
8. von Kries J. Influence of adaptation on the effects produced by luminous stimuli. In: MacAdam DL, editor. *Sources of Color Science*. Cambridge, MA: MIT Press; 1970. p 109–119.
9. Nieves JL, Romero J, García JA, Hita E. Visual system's adjustments to illuminant changes: Heuristic-based model revisited. *Vision Res* 2000;40:391–399.
10. Judd DB, MacAdam DL, Wyszecki G. Spectral distribution of typical daylight as a function of correlated colour temperature. *J Opt Soc Am* 1964;54:1031–1041.
11. Hernández-Andrés J, Romero J, Nieves JL, Lee RL, Jr. Color and spectral analysis of daylight in southern Europe. *J Opt Soc Am A* 2001;18:1325–1335.
12. Borges C. Trichromatic approximation method for surface illumination. *J Opt Soc Am A* 1991;8:1319–1323.
13. Funt BV, Lewis BC. Diagonal versus affine transformations for color correction. *J Opt Soc Am A* 2000;17:2108–2112.
14. Finlayson GD, Funt BV, Jiang H. Predicting cone quantum catches under illuminant change. *Proceedings Eleventh Color Imaging Conference CIC'11*, Scottsdale, 2003. p 160–165.
15. Finlayson GD, Drew MS, Funt BV. Spectral sharpening: sensor transformations for improved color constancy. *J Opt Soc Am A* 1994;11:1553–1563.
16. West G, Brill MH. Necessary and sufficient conditions for von Kries chromatic adaptation to give color constancy. *J Math Biol* 1982;15: 249–258.
17. Drew MS, Finlayson GD. Multispectral processing without spectra. *J Opt Soc Am A* 2003;20:1181–1193.
18. ColorChecker DC. Chart from GretagMacbeth Ltd. (“GMB”), © 2004.
19. Vrhel MJ, Gershon R, Iwan LS. Measurement and analysis of object reflectance spectra. *Color Res Appl* 1994;19:4–9.
20. Tominaga S, Wandell BA. Natural scene-illuminant estimation using the sensor correlation. *Proc IEEE* 2002;90:42–56.
21. CIE. Colorimetry. CIE Tech. Rep. No. 15.2. Vienna: Central Bureau of the CIE; 1986. p 70–72.
22. Smith VC, Pokorny J. Spectral sensitivity of the foveal cone photopigments between 400 and 500 nm. *Vision Res* 1975;15:161–171.
23. Lovell PG, Tolhurst DJ, Párraga CA, Baddeley R, Leonards U, Troscianko J, Troscianko T. Stability of the color-opponent signals under changes of illuminant in natural scenes. *J Opt Soc Am A* 2005;22:2060–2071.